Nonlinear high-frequency hopping conduction in two-dimensional arrays of Ge-in-Si quantum dots: Acoustic methods

I. L. Drichko,[1] A. M. Diakonov,[1] V. A. Malysh,[1] I. Yu. Smirnov,[1] E. S. Koptev,[2]
A. I. Nikiforov,[2] N. P. Stepina,[2] Y. M. Galperin,[3,4,1] and J. Bergli[3]

[1]*A. F. Ioffe Physico-Technical Institute of Russian Academy of Sciences, 194021 St. Petersburg, Russia*
[2]*Institute of Semiconductor Physics, Siberian Branch of Russian Academy of Sciences, 630090 Novosibirsk, Russia*
[3]*Department of Physics, University of Oslo, PO Box 1048 Blindern, 0316 Oslo, Norway*
[4]*Centre for Advanced Study, Drammensveien 78, 0271 Oslo, Norway*

(Dated: February 27, 2013)

Using acoustic methods we have measured nonlinear AC conductance in 2D arrays of Ge-in-Si quantum dots. The combination of experimental results and modeling of AC conductance of a dense lattice of localized states leads us to the conclusion that the main mechanism of AC conduction in hopping systems with large localization length is due to the charge transfer within large clusters, while the main mechanism behind its non-Ohmic behavior is charge heating by absorbed power.

PACS numbers: 81.07.Ta, 62.25.Fg

INTRODUCTION

Nonlinear hopping conduction in various materials and devices was extensively studied, see, e.g., [1, 2] and references therein. Despite relatively large amount of experimental and theoretical work aimed at nonlinear phenomena in static (DC) hopping conduction, the understanding in this research area is far from being complete. The common knowledge is that nonlinear effects in hopping conduction are determined by interplay between the so-called field effects (field-induced deformation of percolation paths governing the conduction) and heating of the charge carriers. The non-Ohmic effects are usually expressed in terms of the dimensionless ratio $eE\mathcal{L}/kT$, where e is the electron charge, E is the electrical field strength, T is the temperature, k is the Boltzmann constant, while $\mathcal{L}$ is some characteristic length. Theoretical considerations [3] based on different models lead to apparently similar predictions: non-Ohmic effects become noticeable at $eE\mathcal{L}/kT \gtrsim 1$. However, predictions of both magnitude $\mathcal{L}$ and its temperature dependence significantly differ. Interplay between the field and the heating effects in DC non-Ohmic hopping conduction is essentially dependent on the relation between the localization length ξ and a typical distance between electrons [1]. In two-dimensional (2D) systems with large localization length the hopping regime is qualitatively different in many respects from the conventional hopping in systems with a small ξ [4]. In particular, the nonlinear effects in the 2D hopping transport in systems with a large ξ are caused by *electron heating* [1].

Much less attention has been paid to non-Ohmic effects caused by a high-frequency (AC) field. Most studies have been done on modifications of DC conductance under electromagnetic radiation. They revealed a rather complicated picture of nonlinear behaviors (see [2] and references therein), which requires more theoretical effort for complete understanding.

High-frequency hopping conductance is conventionally analyzed within the framework of the so-called *two-site model*, according to which an electron hops between states with close energies localized at two different centers. These states form pair complexes, which do not overlap. Therefore, they do not contribute to the DC conduction, but are important for the AC response. Being very simple, the two-site model has been extensively studied, see for a review [5–7] and references therein. As is well known [6], there are two specific contributions to the high-frequency absorption. The first contribution, the so-called resonant, is due to direct absorption of microwave quanta accompanied by interlevel transitions. The second one, the so-called relaxation, or phonon assisted, is due to phonon-assisted transitions, which lead to a lag of the levels populations with respect to the microwave-induced variation in the interlevel spacing. The relative importance of the two mechanisms depends on the frequency ω, the temperature T, as well as on sample parameters. The most important of them is the relaxation rate $\gamma(T)$ of symmetric pairs with interlevel spacing $\sim kT$. At $\omega \lesssim \sqrt{\gamma kT/\hbar}$ the relaxation contribution to the real part of AC conductivity $\sigma_1(\omega)$ dominates. In this case the imaginary component of AC condutivity $\sigma_2 \gtrsim \sigma_1$, and $\sigma_1(\omega) \propto \omega$ with logarithmic accuracy. According to the two-site model, the non-Ohmic conductance *decreases* with the field amplitude [7, 8].

In this work we study nonlinear AC conductance in the samples containing dense arrays of Ge-in-Si quantum dots (QDs) using probe-free acoustic method [9]. We will show that AC conduction of dense QD arrays is similar to that in hopping semiconductors with large localization length.

EXPERIMENT

Samples We study B-doped arrays of Ge-in-Si QDs with densities $n = (3-4) \times 10^{11}$ cm^{-2} and filling factors $\nu \approx 2.5$ - 2.85 [10]. The samples were grown by Stranski-Krastanov molecular beam epitaxy on a (001) Si substrate. The QD array layer was located at 40 nm from the sample surface, see the sketch in the left panel of Fig. 1. QDs are shaped as pyramids with a height of 10-15 Å and a square base having the side of 100-150 Å. The samples were δ-doped with B, the density in the doped layer being $\sim 10^{12}$ cm^{-2}. In these systems two lowest states in Ge QDs are occupied by holes, and the third level is partly occupied. The 4th state is split from the 3rd one by 18-23 meV [11]. Therefore, the 4th level is expected to be empty in the temperature domain of interest.

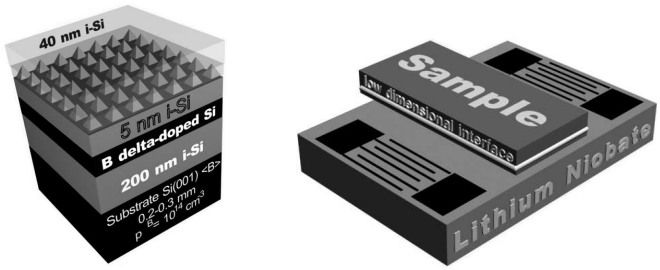

FIG. 1: Sketch of the sample (left) and experimental setup (right).

We studied AC conductance of two samples, which were annealed and were close in conductance. The aim of annealing was increasing of the sample conductance; during the annealing the dots spread and the distance between them decreases from initial ∼15 nm to almost overlapping. The samples studied in [12] had larger conductance and therefore AC hopping conductance was not observed there.

Procedure We used the probeless acoustic method to determine the complex ac conductance, $\sigma \equiv \sigma_1 - i\sigma_2$, from attenuation, Γ, and velocity, V, of a surface acoustic wave (SAW) induced on the surface of a $LiNbO_3$ piezoelectric crystal by interdigital transducers, see right panel of Fig. 1. The sample is pressed to the crystal surface by a spring. A SAW-induced AC electric field penetrates into the sample and interacts with charge carriers (holes). As a result, both Γ and V acquire additional contributions, which can be related to complex σ [9]. We single out these contributions by measuring the changes induced by external transverse magnetic field, $\Delta\Gamma(B) \equiv \Gamma(0) - \Gamma(B)$, and similarly $\Delta V(B)$. For these particular samples ΔV is not measurable thus indicating that $\sigma_2 \ll \sigma_1$. Therefore, further we will discuss only $\Delta\Gamma$ and σ_1. Since the hole absorption vanishes in very high magnetic fields we extrapolate experimentally found $\Delta\Gamma(B)$ to $B \to \infty$ and in this way find $\Gamma(0) \equiv \Gamma$ versus temperature and SAW frequency at frequencies 30-414 MHz in the temperature domain 1.8-13 K.

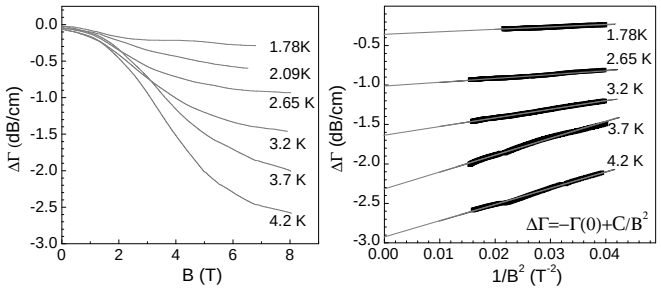

FIG. 2: Left – Magnetic field dependence of $\Delta\Gamma$ at frequency 143 MHz for different temperatures shown at the curves. Right –The same dependences replotted as function of B^{-2}. Sample 1.

Linear regime Shown in the left panel of Fig. 2 are magnetic field dependences of $\Delta\Gamma$ at $f = 143$ MHz and $B \leq 8$ T for different temperatures. These dependences are replotted in the right panel as functions of B^{-2}, which can be represented as straight lines. The attenuation coefficient at $B = 0$, Γ, is determined by crossing of these lines with the axis $B^{-2} = 0$. For the situation relevant to present experiment the general expression [9] relating Γ with $\sigma_1(\omega)$ can be simplified as

$$\Gamma\,(\mathrm{dB/cm}) = 4.34 K^2 q A(q)\, 4\pi t(q)\, \sigma_1(\omega)/\varepsilon_s V\,. \qquad (1)$$

Here $q \equiv \omega/V$ is the SAW wave vector, K is the piezoelectric coupling constant in the $LiNbO_3$, $A(q)$ and $t(q)$ are geometric factors given in [9], which depend on the dielectric constants of the sample (ε_s), vacuum (ε_0) and substrate (ε_1), as well as on the depth of the QD layer and the clearance a between the sample and substrate. The above expression is valid provided $\sigma_2 \ll \sigma_1 \ll \varepsilon_s V/4\pi t(q)$ that is the case in the present situation.

Shown in the left panel of Fig. 3 are temperature dependences of σ_1 for the sample 1 at frequencies 30.1 and 307 MHz found from Eq. (1). The clearance a was determined from Newton's rings. Frequency dependence of Γ for the sample 2 at $T = 4.2$ K is shown in the right

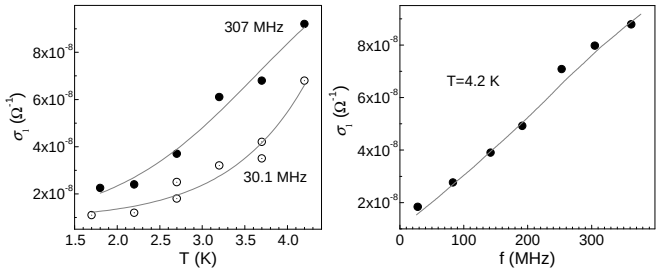

FIG. 3: Left - Temperature dependences of $\sigma_1(\omega)$ in the sample 1 for $f = 30.1$ and 307 MHz. $a = 5 \times 10^{-5}$ cm. Right – Frequency dependence of σ_1 in the sample 2 at $T = 4.2$ K. $a = 4 \times 10^{-5}$ cm. The lines are guides to the eye.

panel.

Nonlinear regime Shown in the left panel of Fig. 4 are magnetic field dependences of $\Delta\Gamma$ at frequency $f = 253$ MHz at $T = 1.8$ K for different input SAW intensities. Similarly to the linear regime, the values $\Gamma(0)$, and σ_1 were determined by extrapolation to $B\to\infty$. The intensities W were determined as follows. Firstly, the signal having passed through the system was compared with the input signal from the generator. This comparison allowed determining the transformation losses in both transducers plus the losses in input and output transmission lines (which are considered to be equal). The intensity was changed by synchronous changing of the calibrated attenuators installed after the generator and after the output transducer keeping the summary attenuation (in dB) constant. Knowing the transformation losses in one transducer and in the input line we find the acoustic intensity after the input transducer. Similar measurements were done for $f = 30$, 143 and 253 MHz.

Since for each frequency the inequality $\Gamma L \ll 1$ (where Γ is the attenuation coefficient in cm^{-1} while $L = 4 - 5$ mm is the sample length) is met, one can neglect the difference between the input and output intensities while calculating the typical amplitude E of the SAW-induced electrical field. It is evaluated from the energy conservation law $2\Gamma W = \sigma_1(E)E^2/2$. This procedure is valid since due to the inequality $\Gamma L \ll 1$ higher harmonics of the signal are weak. The obtained in this way dependence $\sigma_1(E)$ for sample 1, at $T = 1.7$ K and different frequencies is shown on the right panel of Fig. 4. One observe very weak frequency dependence.

The regime of weak non-Ohmic behavior ($E \leq 100$ V/cm) was investigated in more detail for the sample 2 at $f = 142$ MHz and different temperatures, $T = 3$, 3.3, 4.2 and 7 K. The dependences $\Delta\sigma/\sigma_1(0) \equiv [\sigma_1(E)/\sigma_1(0) - 1]$ on dimensionless parameter $(eE\mathcal{L}/kT)^2$ are shown in Fig. 5. The characteristic length $\mathcal{L}$ is chosen as 7.5×10^{-6} cm in order to have $\Delta\sigma/\sigma_1(0) = 1$ at $(eE\mathcal{L}/kT)^2 = 1$. One observes an approximate data collapse.

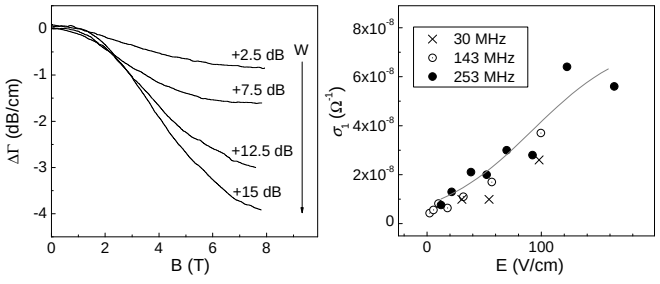

FIG. 4: Left – Magnetic field dependences of $\Delta\Gamma$ at frequency $f = 253$ MHz at $T = 1.8$ K for different input SAW intensities. Right – The dependence $\sigma_1(E)$ for $T = 1.8$ K with the line guided to the eye. Sample 1.

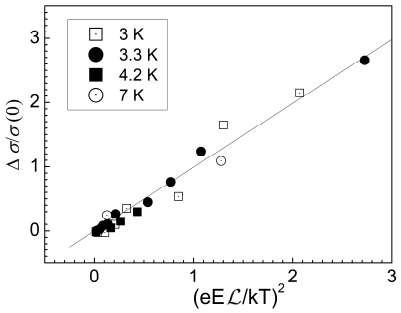

FIG. 5: Dependence of $\Delta\sigma/\sigma_1(0)$ on the dimensionless parameter $(eE\mathcal{L}/kT)^2$. Here $\Delta\sigma(E) \equiv \sigma_1(E) - \sigma_1(0)$, while $\mathcal{L}$ is a characteristic length chosen as 7.5×10^{-6} cm. $f = 142$ MHz , $T = 3$, 3.3, 4.2 and 7 K. Sample 2. The line is guide to the eye.

SIMULATIONS

Since we are not aware of any analytical theory for AC hopping conduction in dense QD arrays we have performed numerical simulations for a model system consisting of a $L \times L$ square lattice of randomly occupied localized states [13]. We put $L = 100$ having in mind that for this size we know that finite size effects are not appreciable in DC conductance [14]. Each of the states can be either empty or occupied (double occupancy is not allowed). The simulations were performed for the filling factor of 1/2, so that the number of electrons is half the number of sites. Disorder is introduced by assigning a random energy in the range $[-U, U]$ to each site (in our numerics we have used $U = e^2/d$ where d is the lattice constant). Each site is also given a compensating charge νe so that the overall system is charge neutral. The charges interact via the Coulomb interaction. In the following the unit of energy is chosen as the Coulomb energy of unit charges on nearest neighbor sites, e^2/d. The unit of temperature is then e^2/dk.

To simulate the time evolution we used the dynamic Monte Carlo method introduced in Ref. [15] for simulating DC transport. The only difference is that we apply an AC electric field $E = E_0 \cos\omega t$ and that, following Ref. [16], we use for the transition rate of an electron from site i to site j the formula

$$\gamma_{ij} = {\tau_0}^{-1} e^{-2r_{ij}/\xi} \min\left(e^{-\varepsilon_{ij}/kT}, 1\right) \qquad (2)$$

where ε_{ij} is the energy of the phonon and r_{ij} is the distance between the sites. τ_0 contains material dependent and energy dependent factors, which we approximate by their average value; we consider it as constant and its value, of the order of 10^{-12} s, is chosen as our unit of time. Consequently, ω is measured in units of τ_0^{-1} while the electric field is measured in units of e/d^2 . The conductance (in Siemens) is expressed in units of $4\pi\epsilon_0 d/\tau_0$. Note that our model is oversimplified comparing to real-

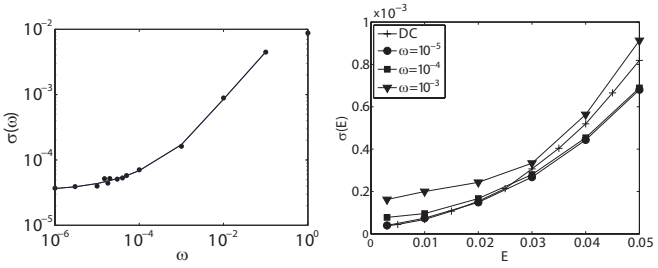

FIG. 6: AC conductivity as function of frequency (left panel) and of electrical field (right panel) for $T = 0.03$.

istic dense QD arrays. In particular, the model assumes a hydrogen-like wave function with localization length ξ and independent of the phonon wave vector electron-phonon coupling, we ignore dielectric susceptibility of the host, etc. Therefore, we hope to reproduce the behavior of AC conductance only qualitatively. However, we believe that the model reproduces main physics of the dense arrays – interplay between Coulomb correlations and disorder as well as relatively large ratio between ξ and a distance between the dots. To decrease the number of independent parameters we put $\xi = d$.

Shown in Fig. 6 (left panel) is the conductance versus frequency for $T = 0.03$ (corresponding to the Efros-Shklovskii regime) and $E_0 = 0.003$ which we know is close to the upper limit of the Ohmic regime for DC transport [14]. Dependences of σ on the field amplitude for different frequencies are shown in the right panel. As it is seen, the conductance grows with frequency, as well as with electric field that qualitatively agrees with the experimental results shown in Figs. 3, 4 (right panels).

We can present the results in a different form: assuming that the non-Ohmic behavior is due to heating of the charge carriers we would expect that the conductance at a large field will be the same as the Ohmic conductance at a *higher* temperature corresponding to the electron temperature. This is known to be approximately true for DC conductivity [14, 17]. Thus, we expect a relation of the form

$$\sigma(T_{\rm eff}, E, \omega) = \sigma(T, 0, \omega) \qquad (3)$$

where $T_{\rm eff}(E)$ is the effective electron temperature while $\sigma(T, 0, \omega)$ is the Ohmic AC conductance. In the simulations we can check the accuracy of this relation by independent calculation of $\sigma(\omega)$ and $T_{\rm eff}$. The latter was found from direct fitting of the Fermi function to the actual distribution function of occupied sites obtained by averaging over 20 states. We also found the Ohmic conductivity as function of temperature for different frequencies. If relation (3) holds we should find at a given frequency the following: as the electric field is increased, both the effective temperature and the conductivity increase in such a way that the points $\sigma(T, E, \omega)$ follow the same curve as the Ohmic conductivity. We plot σ versus $1/\sqrt{T_{\rm eff}}$ for different frequencies in Fig. 7 (left panel). As we can see, relation (3) is approximately satisfied. Therefore, we have used it as a *definition* of the

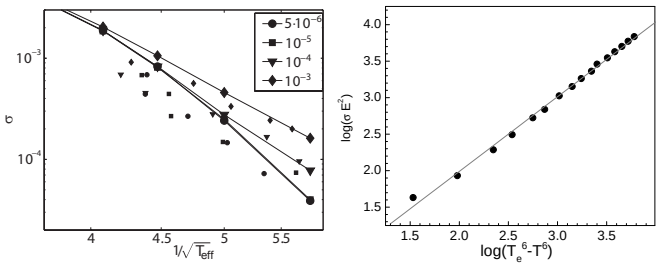

FIG. 7: Left – Conductance as a function of $1/\sqrt{T_{\rm eff}}$ for various frequencies. The large symbols connected by lines show the ohmic conductivity (for which $T_{\rm eff} = T$). The small symbols show the non-Ohmic conductivity at a finite field. Each symbol corresponds to a different frequency. Right – Relationship between $\sigma(T, E)E^2$ and $T_{\rm eff}^6 - T^6$ for sample 1 at $T = 1.8$ K.

electron temperature allowing us to extract it from experimental data on $\sigma(T, E, \omega)$ and $\sigma(T, 0, \omega)$. Shown in the right panel of Fig. 7 is the relationship between so-defined $T_{\rm eff}$ and the absorbed power, $\sigma(T, E, \omega)E^2$, for the lattice temperature of 1.8 K. Here we used averaged data for different frequencies since the frequency dependence is rather weak. The results are compatible with the dependence $T_{\rm eff}^6 - T^6 \propto \sigma(T, E)E^2$. Interestingly, a similar dependence was reported for amorphous InO_x films, which are on the dielectric side of a insulator-to-superconductor transition [18]. Though such a dependence was predicted for a metallic state [19], we are not aware of any analytical theory explaining such a dependence in the insulating phase.

Conclusion Using acoustic methods we have measured real part of nonlinear AC conductance in insulating 2D arrays of Ge-in-Si QDs. The observed features – inequality $\sigma_1 \gtrsim \sigma_2$, increasing of σ_1 with the field amplitude, its relatively weak frequency dependence, large energy exchange length $\mathcal{L} \gtrsim 1/\sqrt{n}$ – essentially *contradict* to the predictions of the two-site model discussed in Sec. . The dissipation is rather due to electron transitions in multi-site clusters. This is not surprising because the two-site model requires the close pairs to be isolated that can be met only in dilute systems. The observed non-Ohmic behavior is attributed to *heating* of the charge carriers by AC electrical field, as in the DC case [1]. We have also performed simulations of AC conductance in a dense 2D lattice of localized states taking into account both distribution of their energies and Coulomb correlations. The results qualitatively agree with experiment confirming the above conclusion.

This work was supported by grant of RFBR 11-02-00223, grant of the Presidium of the Russian Academy of

Science, the Program "Spintronika" of Branch of Physical Sciences of RAS.

[1] M. E. Gershenson, *et al.* Phys. Rev. Lett. **85**, 1718 (2000).

[2] Z. Ovadyahu, Phys. Rev. B **84**, 165209 (2011).

[3] R. M. Hill, Philos. Mag. **24**, 1307 (1971); B. I. Shklovskii, Fiz. Tekh. Poluprovodn. **6**, 2335 (1972) [Sov. Phys. Semicond. **6**, 1964 (1973)]; N. Apsley and H. P. Hughes, Philos. Mag. **31**, 1327 (1975); M. Pollak and I. Riess, J. Phys. C **9**, 2339 (1976); B. I. Shklovskii, Fiz. Tekh. Poluprovodn. **10**, 1440 (1976) [Sov. Phys. Semicond. **10**, 855 (1976)]; B. I. Shklovskii, Fiz. Tekh. Poluprovodn. **13**, 93 (1979); I. P. Zvyagin, Phys. Status Solidi B 88, 149 (1978).

[4] B. I. Shklovskii and A. L. Efros, *Electron properties of dopes semiconductors* (Springer Verlag, Berlin, 1984).

[5] A. L. Efros, Zh. Eksp. Teor. Fiz. **89**, 1834 (1985) [Sov. Phys. JETP **62**, 1057 (1985).

[6] A. L. Efros and B. I. Shklovskii, in *Electron-Electron Interactions in Disordered Systems*, edited by A. L. Efros and M. Pollak (North-Holland, Amsterdam, 1985), p. 409.

[7] Y. M. Galperin, V. L. Gurevich and D.A. Parshin, in *Hopping Transport in Solids*, edited by B. Shklovskii and M. Pollak (Elsevier, NY, 1991).

[8] Y. M. Galperin, M. Kirkengen, Phys.Rev.B **56**, 13615 (1997); *ibid.* **62**, 16624 (2000).

[9] I. L. Drichko, A. M.Diakonov, I. Yu. Smirnov, Y. M. Galperin and A.I.Toropov, Phys. Rev. B **62**, 7470 (2000).

[10] N. P. Stepina, E. S. Koptev, A. V. Dvurechenskii and A. I. Nikiforov, Phys.Rev. B **80**, 23 (2010).

[11] A. I. Yakimov, *Electronic phenomena in Ge-in-Si quantum dot arrays* (in Russian), Dr. Sci. thesis, Novosibirsk (2001).

[12] I. L. Drichko, A. M. Dyakonov, I. Yu. Smirnov, A. V. Suslov, Y. M. Galperin, A. I. Yakimov and A. I. Nikiforov, Zh. Eksp. Teor. Fiz. **128**, 1279 (2005) [Sov. Phys. JETP **101**, 1122 (2005)].

[13] J. H. Davies, P. A. Lee, and T. M. Rice, Phys. Rev. Lett. **49**, 758 (1982).

[14] A. Voje, MD thesis, UiO (2009), http://urn.nb.no/URN:NBN:no-26080.

[15] D. N. Tsigankov and A. L. Efros, Phys. Rev. Lett. 88, 176602 (2002).

[16] K. Tenelsen and M. Schreiber, Phys. Rev. B **52**, 13287 (1995). A. Díaz-Sánchez et. al., Phys. Rev. B **59**, 910 (1999).

[17] M. Caravaca, A. M. Somoza, M. Ortuño Phys. Rev. B **82**, 134204 (2010).

[18] M. Ovadia, B. Sacépé, and D. Shahar, Phys. Rev. Lett. **102**, 176802 (2009).

[19] A. Schmid, Z. Phys. **271**, 251 (1974); M. Reizer and A. Sergeyev, JETP **63**, 616 (1986).